Am J Transl Res 2015;7(11):2291-2304
www.ajtr.org /ISSN:1943-8141/AJTR0012948

Original Article

Dysregulated expression of microRNAs and mRNAs in myocardial infarction

Yaping Wang[1,2], Xiaohong Pan[1], Youqi Fan[1], Xinyang Hu[1,2], Xianbao Liu[1,2], Meixiang Xiang[1,2], Jian'an Wang[1,2]

[1]Department of Cardiology, Second Affiliated Hospital, College of Medicine, Zhejiang University, Hangzhou 310009, PR China; [2]Key Lab of Cardiovascular Disease, Second Affiliated Hospital, College of Medicine, Zhejiang University, Hangzhou 310009, PR China

Received July 15, 2015; Accepted October 31, 2015; Epub November 15, 2015; Published November 30, 2015

Abstract: Acute myocardial infarction (AMI) is a major cause of mortality in the general population. However, the molecular phenotypes and therapeutic targets of AMI patients remain unclear. By profiling genome-wide transcripts and microRNAs (miRNAs) in a cohort of 23 AMI patients and 23 non-AMI patients, we found 218 dysregulated genes identified in the infarcted heart tissues from AMI patients relative to non-AMI controls. Pathway enrichment analysis of the dysregulated genes pointed to cell signaling/communication, cell/organism defense and cell structure/motility. We next compared the expression profiles of potential regulating miRNAs, suggesting that dysregulation of a number of AMI-associated genes (e.g., *IL12A*, *KIF1A*, *HIF1α* and *CDK13*) may be attributed to the dysregulation of their respective regulating miRNAs. One potentially pathogenic miRNA-mRNA pair, miR-210-*HIF1α*, was confirmed in a mouse model of myocardial infarction (MI). Inhibition of miR-210 expression improved the survival and cardiac function of MI mice. In conclusion, we presented the pathologic relationships between miRNAs and their gene targets in AMI. Such deregulated microRNAs and mRNAs like miR-210 serve as novel therapeutic targets of AMI.

Keywords: Acute myocardial infarction, gene expression, microRNAs, hypoxia-inducible factor 1

Introduction

Acute myocardial infarction (AMI) causes approximately two million deaths per year. In US, approximately 500,000 episodes of AMI occur per year. Around 600/100,000 men and 200/100,000 women have AMI each year [1]. AMI occurs when blood stops flowing properly to a part of the heart, and the heart muscle is injured because it is not receiving enough oxygen [2]. Usually this is because one of the coronary arteries that supplies blood to the heart develops a blockage due to an unstable build-up of white blood cells, cholesterol and fat [2]. In the acute phase of AMI increased leukocyte count, a non-specific marker of inflammation, is the risk factor for future cardiovascular events and predicts mortality in those with STEMI [ST-segment elevation MI] and NSTEMI (non-STEMI) [3, 4]. Obtaining novel insights into the pathophysiology of myocardial infarction (MI) should aid the discovery of novel biomarkers and elaboration of novel therapeutic strategies.

MicroRNAs (miRNAs) regulate gene expression post-transcriptionally by base-pairing to partially complementary sequences in target messenger RNAs (mRNAs) [5]. Impairment of the miRNA pathway in cardiac muscle leads to heart failure and cardiomyopathy [6, 7]. Furthermore, altered miRNA expression patterns have been associated with various cardiac pathologies [8-10]. However, the functional specificity for miRNAs as biomarkers of MI is still lacking. On the other hand, several miRNAs are with tissue specific expression (e.g., the miR-133 family), and therefore there are high expectations to identify more-specific markers that can be used as early stage markers of myocardial necrosis. A substantial of differential genes were examined when response to MI [11, 12]. Integrating the mRNA and miRNA profiles, therefore, could help to elucidate the mechanisms in MI development and provide novel biomarkers for the outcomes of AMI. Here, we searched for the enriched pathways among the dysregulated genes associated with AMI and we further demonstrated that miRNAs could potentially play a

critical role in determining the gene expression dysregulation observed in AMI patients.

Materials and methods

Subjects

Patients clinically diagnosed with AMI were included from Department of Cardiology, Second Affiliated Hospital, School of Medicine Zhejiang University from 2011 to 2013. We sought to include consecutive patients that agreed to participate in the study (Table S1). Our study included autopsy samples of infarcted heart tissue and border zone from 23 patients with MI. MI was diagnosed clinically by symptoms and/or electrocardiographic changes, and confirmed by elevated plasma levels of markers of cardiac necrosis. All the patients underwent coronary angiography and angioplasty of infarct related artery. Autopsies were performed within 24 hours after death. Tissue samples were fixed in 10% buffered formalin and embedded in paraffin. The duration of MI at the time of death was estimated on the basis of histological changes and clinical data. Pharmacological treatment was according to current guidelines [13]. There is no significant difference on the pharmacological treatment and procedures underwent by the patients. The non-AMI control group consisted of autopsy heart tissue from 23 healthy adults who had died in accidents. Post mortem delay did not exceed 24 hours, and there was no macroscopical or microscopical evidence of disease at autopsy. All the subjects in the control group have no history of myocardial infarction. The study was approved by the Ethics Review Board of College of Medicine, Zhejiang University. All patients or their guardians gave written informed consent, and conformed to the tenets of the Declaration of Helsinki.

Microarray analysis

Tissue samples were cut at 10 μm from formalin fixed paraffin-embedded tissue blocks using a microtome. Six to eight 10-μm sections were used for the isolation procedure. Total RNA isolation was performed using a miRNeasy FFPE kit (Qiagen) according to the manufacturer's protocol. RNA concentration and purity was determined and before gene expression profiling (Affymetrix Human Exon 1.0ST Array). The microarray labeling, hybridization and processing was performed according to the manufacturer's protocol at the Microarray Core Facility of Chinese National Human Genome Center, Shanghai, China. The raw data of microarray were quantile-normalized over all samples, summarized with the robust multi-array average (RMA) algorithm [14] and log2 transformed with a median polish [15] for ~22,000 transcript clusters (gene-level) [16]. Significance Analysis of Microarrays (SAM) [17] was used to identify differential genes between AMI patients and non-AMI controls. Microarray data are available in the Array Express with the identification of Array Express accession: E-MTAB-3573.

Pathway analysis

Enriched pathways and biological processes among the differential genes were performed using the DAVID (Database for Annotation, Visualization and Integrated Discovery) tool [18, 19]. The following databases were included: KEGG (Kyoto Encyclopedia of Genes and Genomes) [20] and Gene Ontology (GO) [21].

miRNA expression profiling

The TaqMan Low-Density Array Human MicroRNA Panel v1.0 (Applied Biosystems, Foster City, CA, USA) was utilized for global miRNA profiling. The panel includes two 384-well microfluidic cards (human miRNA pool A and pool B) that contain primers and probes for 746 different human miRNAs in addition to six small nucleolar RNAs that function as endogenous controls for data normalization. Briefly, equal quantity of RNA (30 ng) from the infarcted heart tissues from 23 patients with AMI as well as 23 non-AMI controls was pooled and reverse transcribed for cDNA synthesis using the TaqMan Multiplex RT set (Applied Biosystems) for TaqMan Array Human MicroRNA Panels. Each RT reaction was diluted 62.5-fold with water and 55 μL of each diluted product was combined with 55 μL of TaqMan 2X Universal PCR Master Mix, No AmpErase UNG (Applied Biosystems). One-hundred microliters of the sample/master mix for each Multiplex pool were loaded into fill reservoirs on the microfluidic card. The array was then centrifuged and mechanically sealed with the Applied Biosystems sealer device. Quantitative PCR was performed on an Applied BioSystems 7900HT thermocycler (Applied Biosystems) using the

manufacturer's recommended cycling conditions. Fold changes for each miRNA were normalized to the endogenous control U6. The selection of 23 samples within each group was based upon sample availability and statistical test power. The efficiency of pooling total RNA in microarray experiments was based upon published methods [22] and the RNA pooling enabled us to reduce number of arrays without a loss of precision.

miRNA-mRNA relationships

The expression patterns of those miRNAs and their corresponding gene targets were compared between AMI patients and non-AMI controls using standard *t*-test. Significant miRNA-mRNA relationships (i.e., negative association between miRNA and mRNA at *t*-test $p<0.05$) were further confirmed using linear regression. The Pearson correlation coefficients and the associated *p*-values (cutoff $p<0.05$) were calculated using R Statistical Package.

Quantification of miRNA

MiRNAs were quantified by using TaqMan miRNA qRT-PCR assay according to the protocol of the manufacturer (Applied BioSystems, Inc.). The data were analysed with automatic setting for assigning baseline; the threshold cycle (Ct) is defined as the fractional cycle number at which the fluorescence exceeds the given threshold. The data obtained by real-time PCR were translated in log2 (relative level).

Quantification of messenger RNAs

One microgram of total RNA from the infarcted heart tissues from 10 patients with AMI as well as non-AMI controls was reverse-transcribed in 20-μl reaction with random primers using the SuperScript III first-strand synthesis kit (Life technologies, Carlsbad, CA, USA). For real-time PCR, 1 μl of diluted cDNA (1:20) was amplified for 40 cycles with a master mix (SYBR Green Supermix; Applied Biosystems) using real-time PCR Systems (Bio-Rad, Hercules, CA, USA). Melting curve analysis was done at the end of the reaction to assess the quality of the final PCR products. The threshold cycle C(t) values were calculated by fixing the basal fluorescence at 0.05 unit. Three replicates were used for each sample and the average C(t) value was calculated. The ΔC(t) values were calculated as C(t) sample – C(t) GAPDH. The N-fold increase or decrease in expression was calculated by the ΔΔCt method using the C(t) value as the reference point.

Luciferase assays

H9c2 cells were seeded at 5×10^5 cells per well 24 hr before transfection. Cells were transfected using Lipofectamine 2000 transfection reagent (Life Technologies) with 10 nM miR-210, 1 ng of phRL-TK-HIF1α or phRL-TK-mutHIF1α and 5 ng of firefly luciferase reporter plasmid (pGL3-control) was to normalize transfection efficiency. Luciferase activity was measured 36 hr after transfection by the Dual-Luciferase Reporter Assay System (Promega, Madison, WI).

AntagomiR design

Cholesterol-modified RNA oligonucleotides (antagomiRs) directed against human and murine miR-210 (MIMAT0000658) were designed as described [23] and synthesized by Microsynth (antagomirs, Dharmacon RNA technologies, Lafayette, CO). For antagomir-210 the following sequence was used: 5'-G_sC_s U-CAGCCGCUGUCACACGCACAG $A_sC_sG_sA_s$-Chol-3'. As a negative control, twelve point mutations were introduced into the miR-210 mature sequence (antagomiR_MM as control) creating an RNA sequence that is not encoded in the murine genome. The lower case letters represent 2'-*O*Me-modified nucleotides; subscript 's' represents phosphorothiate linkage; 'Chol' represents a cholesterol-group linked through a hydroxyprolinol linkage. AntagomiR-210 (25 mg/kg) and antagomiR negative control (antagomiR_MM) per animal were injected immediately after LAD ligation into the myocardium bordering the infarct zone (single injection), using an insulin syringe with incorporated 30-gauge needle.

Mouse model of myocardial infarction

All animal procedures were performed in accordance with the regulations of the NIH Office of Laboratory Animal Welfare and were approved by the Institutional Animal Care and Use Committee (IACUC) of College of Medicine, Zhejiang University. Myocardial infarction was produced in C57BL/6 mice (8-12 weeks old), by permanent left anterior descending (LAD) coro-

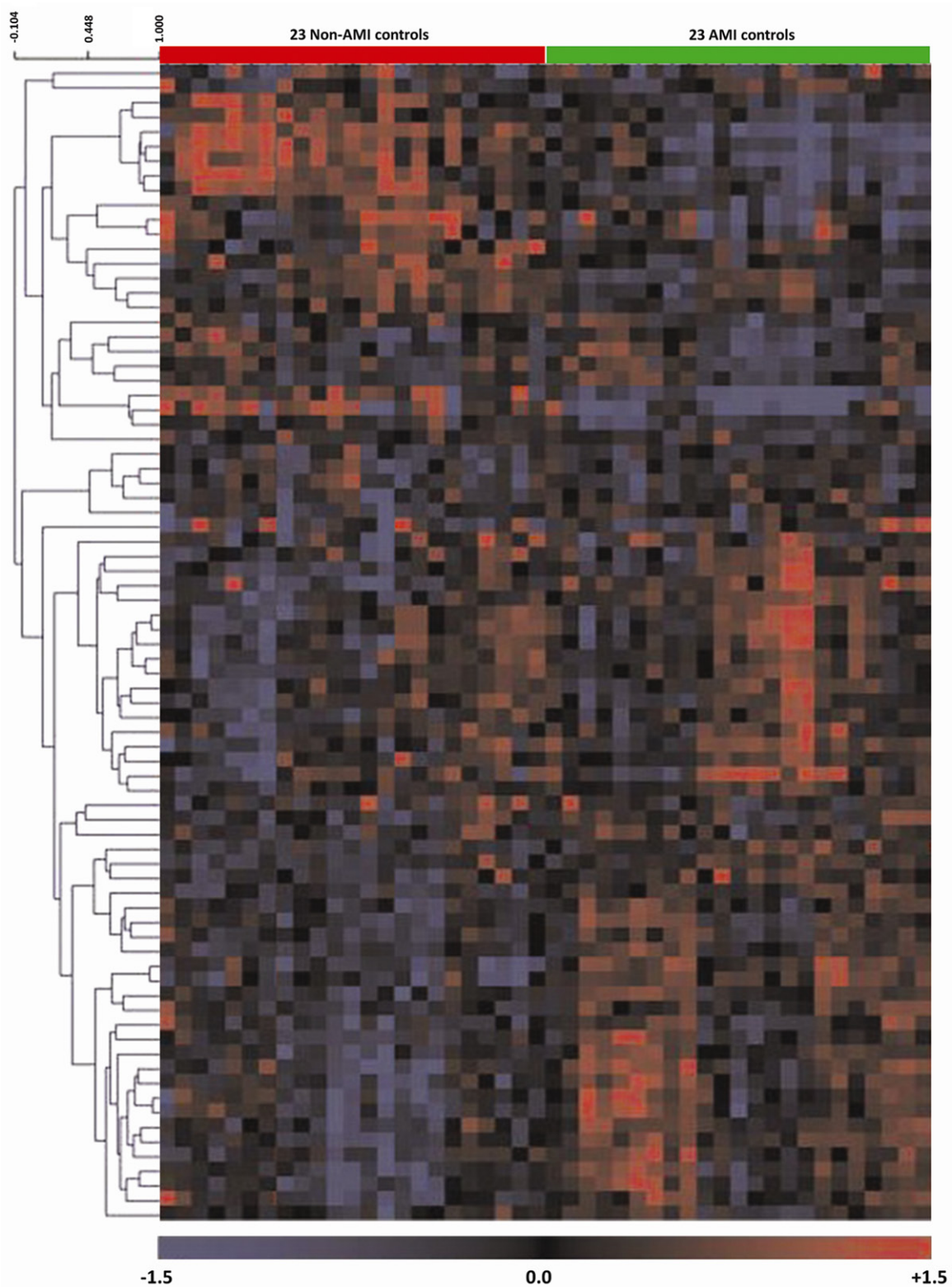

Figure 1. Genes dysregulated (25 up regulated and 55 down regulated genes) in AMI patients. Red represents up-regulation when comparisons of AMI patients to non-AMI controls. Blue represents down-regulation. (left) mRNA clustering tree; (top) AMI and non-AMI samples. Red bars: AMI patients; Green bars: non-AMI controls. Student's t-test was performed to detect differentially expressed miRNAs. Bonferroni procedure was used to calculate adjusted *p* values to control false discovery rate (FDR) among AMI patients and non-AMI controls.

nary artery ligation. Briefly, mice were anesthetized with an intraperitoneally injection of ketamine and xylazine, endotracheally intubated and placed on a rodent ventilator. The beating heart was accessed via a left thoracotomy. After removing the pericardium, a descending branch of the LAD coronary artery was visualized with a stereomicroscope (Leica) and occluded with a nylon suture. Ligation was confirmed by the whitening of a region of the left ventricle, immediately post-ligation. Ultrasonic cardiogram (UCG) was performed on the surviving animals. Hearts were arrested in diastole by intravenous administration of 2 mol/l KCl and collected after UCG for further analysis.

Immunohistochemistry

Five-μm sections were cut, dewaxed with xylene and rehydrated with graded alcohol. The slides were then placed in a 0.01 M citrate buffer solution (pH =6.0) and pre-treatment procedures to unmask the antigens were performed in a microwave oven for 10 minutes. Sections were treated with peroxidase and protein block for 60 min each and then incubated overnight with anti-HIF1α (rabbit anti-mouse polyclonal antibody 1:300, Abcam) antibodies at 4°C. After conjugation with primary antibodies, sections were incubated with biotin-labeled secondary antibody (Thermo Scientific) for 20 minutes at room temperature. Finally, sections were incubated with streptavidin–peroxidase complex for 20 minutes at room temperature (Thermo Scientific), DAB chromogen (Thermo Scientific) added and counter staining done with haematoxylin. For negative control, the primary antibody was not added to sections and the whole procedure carried out in the same manner as mentioned above.

Infarct size determination

The M-mode measurements of LV dimensions were averaged from more than 3 cycles. LV end-systolic diameter (LVESD) and end-diastolic diameter (LVEDD), interventricular septal thickness in diastole (IVSd) and LV posterior wall thickness (LVPWT) were measured. Percent LV fractional shortening (%FS) was calculated as follows: %FS = (LVEDD-LVESD)/LVEDD*100 (%). Percent ejection fraction (%EF): %EF = 100*((LV Vol;d-LV Vol;s)/LV Vol;d); LV Vol;d = ((7.0/(2.4+LVID;d))*LVID;d^3); LV Vol;s = ((7.0/(2.4+LVID;s))*LVID;s^3).

Statistical analysis

All data analysis was performed using R software. We initially designed the experiments to minimize the impact of covariates by matching the samples for key confounding factors. Therefore, we used a univariate test to screen for differentially expressed miRNAs, and validated the result with a separate set of samples. A Student's t-test was performed to detect differentially expressed miRNAs. Bonferroni procedure was used to calculate adjusted *p* values to control false discovery rate (FDR) among AMI patients and non-AMI controls. The association between expression levels of mRNAs and miRNAs was analyzed using the Pearson's correlation. Comparison of parameters between two groups was performed by unpaired Student's t test (when distributions were normal) or Mann-Whitney U test (when distributions were significantly skewed). Statistical significance was defined as $p<0.05$ (two-tailed).

Results

Identifying genes dysregulated in AMI patients

Demographic and clinical outcome data for both AMI and non-AMI subjects are summarized in Table S1. Twenty-three AMI patients and 23 non-AMI healthy controls were included in this pilot study. All baseline clinical characteristics, including age, gender, hypertension, diabetes, current smoking, and body mass index (BMI) showed not significantly different between both groups (Table S1). RNA samples before submission were randomized and assayed on the microarray platform. In total, 218 genes were differentially expressed in the infarcted heart tissues between patients with AMI (n=23) and non-AMI controls (n=23) (fold-change >1.5, *p*-value <0.01) with 153 down-regulated and 65 up-regulated genes (Table S2). A heatmap was generated using the time-dependent differentially dysregulated genes (25 up regulated and 55 down regulated, $p<0.01$, 80 mRNAs) in the infarcted heart tissues from AMI patients (**Figure 1**). These results indicated that there was a substantial change of gene expression in the heart myocardium of AMI patients.

Enriched pathways among dysregulated genes

DAVID analysis on the 218 dysregulated genes in our recruited AMI cases revealed 23 enriched pathways and GO biological processes such as

Table 1. Pathways and biological process were enriched in the dysregulated genes inAMI patients

Pathways	Count	%	*P* Value	Fold Enrichment	Benjamini FDR
Cell signaling/communication	16	7	1.46E-06	3.909	0.001
Induction of apoptosis	33	15	1.86E-06	2.115	0.001
Hemostasis	13	6	2.36E-05	3.729	0.002
Regulation of body fluid levels	12	6	3.69E-05	3.928	0.002
Blood coagulation	20	9	4.42E-05	2.317	0.001
Protein expression	18	8	6.01E-05	2.444	0.001
Coagulation	10	5	8.25E-05	4.632	0.035
Gene expression	10	5	8.25E-05	4.632	0.035
Metabolism	10	5	1.03E-04	4.507	0.022
Cell division	10	5	1.10E-04	4.373	0.004
Wound healing	26	12	1.20E-04	1.958	0.023
Negative regulation of cell proliferation	26	12	1.87E-04	1.902	0.027
Response to endogenous stimulus	10	5	4.67E-04	3.706	0.064
Cell structure/motility	10	5	5.62E-04	3.597	0.061
Cell/organism defense	10	5	5.62E-04	3.597	0.061
Negative regulation of cell communication	10	5	6.92E-04	3.500	0.063
Response to wounding	12	6	7.24E-04	2.809	0.017
Response to lipopolysaccharide	9	4	7.56E-04	3.885	0.059
Response to molecule of bacterial origin	10	5	7.74E-04	3.369	0.017
Immune response	13	6	1.38E-03	2.531	0.090
Response to glucocorticoid stimulus	9	4	1.44E-03	3.531	0.085
Response to corticosteroid stimulus	8	4	2.20E-03	3.723	0.039
Response to extracellular stimulus	8	4	2.31E-03	3.694	0.038
Response to steroid hormone stimulus	8	4	3.50E-03	3.434	0.047
Inflammatory response	6	3	9.15E-03	4.043	0.088

programmed cell death, cell signaling/communication, cell/organism defense, and cell structure/motility (FDR <25%, a minimum of 5 genes). **Table 1** shows the top-ranking pathways and biological processes (FDR <10%, a minimum of 10 genes) for each gene group. In addition, analysis on the 218 potentially AMI-associated genes showed enrichment in pathways such as cell cycle and programmed cell death. Eight known pathways and GO biological processes such as homeostasis and blood coagulation were enriched among the 153 down-regulated genes, while 19 GO biological processes such as cell division, negative regulation of cell proliferation, and response to glucocorticoid stimulus were enriched among the 65 up-regulated genes (**Table 1**).

MiRNAs were differentially expressed in AMI patients compared to non-AMI controls

To identify differentially expressed miRNAs in AMI patients, we profiled the expression of 746 miRNAs using the TaqMan microRNA array. This method involves a stem-loop reverse transcription followed by TaqMan real-time PCR analysis that amplifies only mature miRNA and can discriminate among miRNAs which differ by as few as one nucleotide with high sensitivity and specificity [24, 25]. The total RNA obtained from the infarcted heart tissues from all 23 AMI patients and 23 non-AMI controls was pooled with equal quantity (30 ng). The pooled samples (23 per group) are approximately equivalent to 10-15 independent samples in each group, if samples were not pooled, and also assume a wide range of values for the ratio of biological variations among the samples over the technical variations in the assays [22]. Global miRNA expression profiling was performed using TaqMan Low-density Human MicroRNA Array in combination with Megaplex RT and Megaplex pre-amplification techniques. To investigate the relative abundance of detected miRNAs, they were normalized in each patient to U6. The results identified 333 miRNAs (~44.6%) (Ct values <35 were classed as detectable), indicating that global miRNA

Table 2. The miRNA-mRNA pairs in dysregulated miRNAs and dysregulated mRNAs inAMI patients

Potential regulating miRNAs	Target gene mRNAs	Gene title	*P* value
hsa-miR-1	ZNF280C	zinc finger protein 280C	2.04E-03
hsa-miR-1	KIF2A	kinesin heavy chain member 2A	1.39E-05
hsa-miR-1	TCF7	transcription factor 7, T cell specific	1.41E-03
hsa-miR-210	HIF1A	hypoxia inducible factor 1, alpha subunit	1.63E-03
hsa-miR-210	RUNX3	runt-related transcription factor 3	1.54E-03
hsa-miR-208a	TIMM23	translocase of inner mitochondrial membrane 23 homolog	2.25E-03
hsa-miR-208a	CDYL	chromodomain protein, Y-like	1.53E-04
hsa-miR-148b	EIF2C4	eukaryotic translation initiation factor 2C, 4	8.00E-04
hsa-miR-148b	CDK19	cyclin-dependent kinase 19	1.31E-03
hsa-miR-184	CCL16	chemokine (C-C motif) ligand 16	1.80E-03
hsa-miR-451	CPNE3	copine III	1.74E-03
hsa-miR-302b	TGFBR2	transforming growth factor, beta receptor II	1.73E-03
hsa-miR-302b	NF1	neurofibromin 1	6.47E-05
hsa-miR-499	CCL8	chemokine (C-C motif) ligand 8	1.12E-04
hsa-miR-133a	CDK13	cyclin-dependent kinase 13	2.27E-03
has-miR-99a	mTOR	mechanistic target of rapamycin (serine/threonine kinase)	8.06E-04
hsa-miR-433	IL12A	interleukin 12A	1.27E-03

expression profiling is a feasible method to identify aberrantly expressed miRNAs in AMI patients. Comparison of the miRNA expression profile in AMI patients to non-AMI controls demonstrated that 20 miRNAs were up regulated and 8 miRNAs were down regulated in the AMI group (relative fold >2, $p<0.05$, FDR corrected) (Table S3), suggesting that these miRNAs might be important in AMI pathogenesis.

Potential regulating miRNAs were identified for the dysregulated genes

We searched for potential regulating miRNAs for the dysregulated genes in AMI patients based on the predictions of the miRanda algorithm [26]. A specific negative association between miRNAs and mRNAs was tested using t-test and further confirmed using linear regression using the Pearson correlation coefficients. We firstly evaluated the anti-correlation of miRNAs and mRNAs abundances although it neglected the potential cases in which miRNAs directed mRNA translational suppression. Among the 153 down-regulated genes in these samples, 98 miRNA-mRNA relationships corresponding to 53 expressed miRNAs and 51 genes were identified (miRanda: $p<1.0\times10^{-3}$), while 43 miRNA-mRNA relationships corresponding to 22 expressed miRNAs and 18 genes were identified in the 65 up-regulated genes (miRanda: $p<1.0\times10^{-3}$). In addition, 9 up-regulated miRNAs and 3 down-regulated miRNAs in AMI patients were found to be potentially regulating miRNAs in our miRanda algorithm prediction. **Table 2** lists all the miRNA-mRNA pairs found in potential regulating miRNAs and dysregulated mRNAs in AMI.

We further searched for miRNAs that showed a negatively associated expression pattern with their potential gene targets. For the down-regulated miRNAs in the AMI patients, 14 potential regulating miRNAs were found to be up-regulated in the patients (corresponding to 8 miRNA-mRNA relationships). In order to examine the correlations between potentially regulating miRNAs and their targeting genes, we increased our sample size by adding an independent cohort of 13 AMI patients and 11 non-AMI controls. For example, hsa-miR-1 was over expressed while its potential target, *KIF1A* (encoding kinesin heavy chain member 1A), was down-regulated in the AMI patients; miR-210 was up regulated with inversely down-regulation of *HIF1α* (hypoxia inducible factor 1, alpha subunit) mRNA levels in the AMI patients; and miR-133a was up-regulated in the AMI patients with under expression of its potential target, *CDK13* (encoding cyclin-dependent kinase 13). In contrast, three miRNA-mRNA relationships were identified among the down-regulated miRNAs

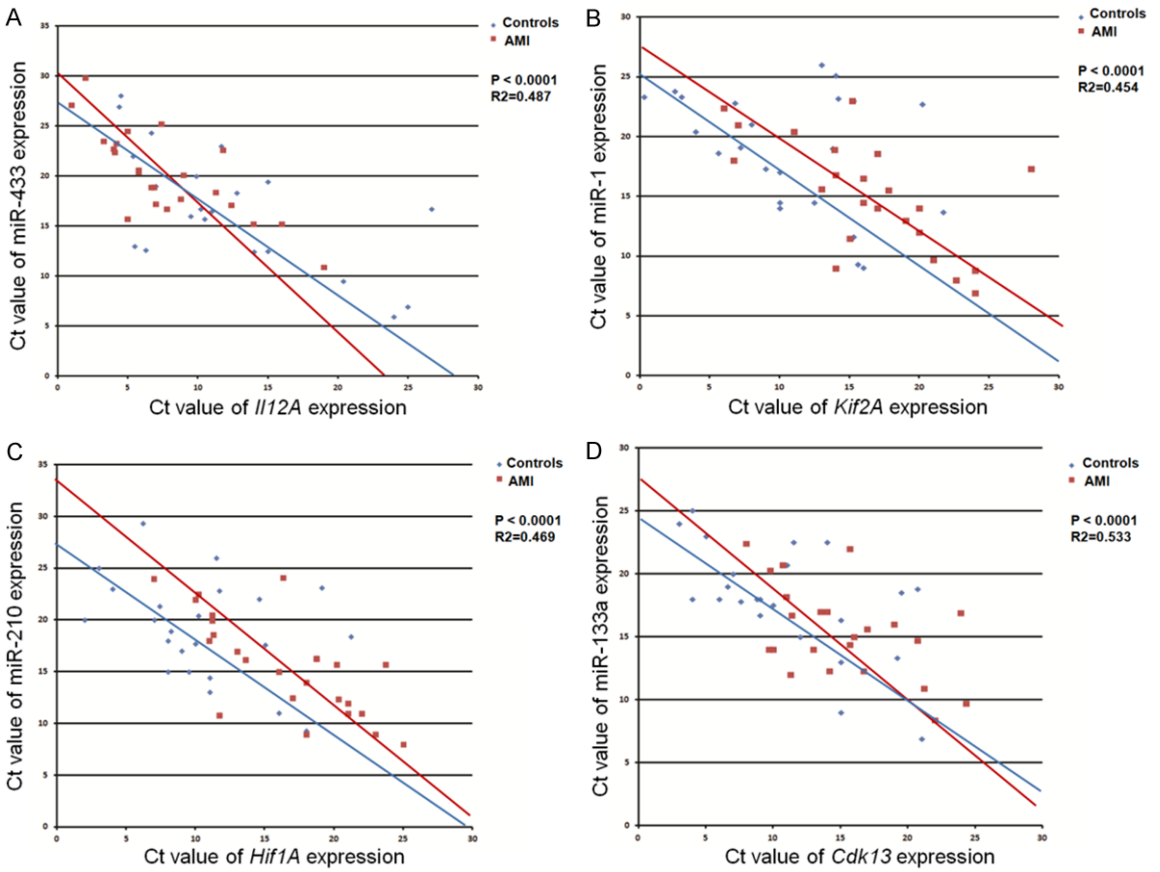

Figure 2. The relationships of potential regulating miRNAs and their dysregulated genes. The association between expression levels of mRNAs and miRNAs was analyzed using the Pearson's correlation. Blue dots represent the non-AMI control samples. Red dots represent the AMI patient samples. X-axis: miRNA expression; Y-axis: mRNA expression. (A) miRNA-433~*IL12A*; (B) miRNA-1~*KIF1A*; (C) miR-210~*HIF1α*; and (D) miRNA-133a~*CDK13*.

in the AMI patients. For example, hsa-miR-433 was down-regulated, while its gene target, *IL12A* (encoding interleukin 12A) was up-regulated in AMI patients. Linear regression confirmed the relationships between miRNAs and their potential gene targets. **Figure 2** shows some examples of the confirmed ($p<0.05$) miRNA-mRNA relationships in the AMI patients. These results demonstrated that a substantial of pathogenic miRNA-mRNA pairs exist at genomic level in AMI patients.

HIF1α is a target of miR-210 in vitro

We next identified potential miR-210 targets by using four algorithms (Target scan, PicTar, miRDB and miRanda) to predict miR-210 targets. We assigned all targets predicted by miRanda scores for an empirical probability of target inhibition through the use of mirSVR scores and a stringent mirSVR score cutoff [27], which clearly demonstrated that there was one binding site of miR-210 to the 3'UTR of *HIF1α* mRNA (**Figure 3A**). To test whether *HIF1α* was a direct target of miR-210, fragments of the 3' UTRs of *HIF1α* containing wild-type or mutated miR-210 complementary sites were cloned into the phRL-TK renilla luciferase reporter plasmid. Luciferase reporters were cotransfected with miRNA mimic of miR-210 into H9c2 cardiac myoblast cells. We then examined binding of human miR-210 to the 3'UTR of *HIF1α* mRNA using a luciferase assay. As the 3'UTR of *HIF1α* is inserted downstream of the luciferase ORF, specific binding to miR-210 prevents luciferase reporter gene expression (**Figure 3B**). In addition, mutations of both *HIF1α* binding sites decreased specific binding to miR-210 and restored luciferase activity (**Figure 3B**) indicating that *HIF1α* is indeed a target of miR-210. These results strongly suggest that over expression of miR-210 in cardiac

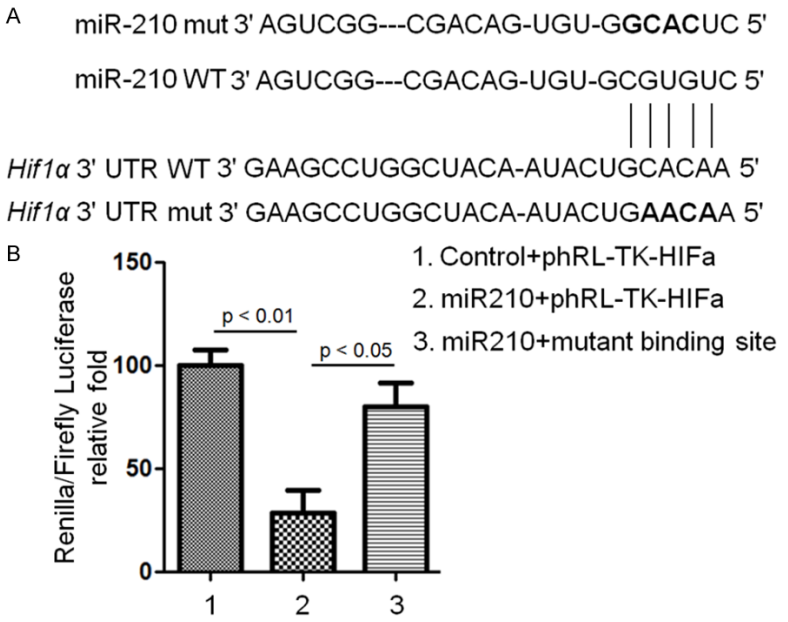

Figure 3. *HIF1α* is a target of miR-210 *in vitro.* A. Sequence alignment of wild-type (WT) and mutated (mut) miR-210 and *HIF1α* 3'UTR; bold indicates mutated sequences in 'seed regions' of miR-210 and *HIF1α*. B. Renilla luciferase activity was normalized to the Firefly luciferase activity. Experiments were repeated in triplicate and data were represented as mean ± SEM compared by Student t test.

myoblasts results in a significant reduction in the levels of *HIF1α*, which indicated that miR-210 might regulate myocardial infarction via HIF1α signal pathway.

Improvement in cardiac function by miR-210 under expression

To investigate whether dysregulated miRNA-mRNA pairs play an important pathogenic role in MI development, we further pursue miR-210~*HIF1α* as example to examine their potential function. We first established the mouse model of MI by coronary artery ligation and knockdown miR-210 *in vivo* using antagomiRs. Heart tissues were collected from the mice at various time points (0, 1, 3, 6, 12, 24 h after coronary artery ligation). The expression profile of miR-210 was markedly increased in the MI group and antagomiR_MM group throughout the 44-day observation period. However, miR-210 expression dramatically decreased in the antagomiR-210 group 24 hrs after infarction and maintained thereafter 20-25% of the miR-210 levels in the AntagomiR group over the 44-day period (Figure S1). The expression of *HIF1α* in the nuclei of endothelial cells of mouse heart was compared. There was a higher nuclear expression of HIF1α by cardiac myocytes and endothelial cells after four weeks of MI when treatment with antagomiR-210 relative to antagomiR_MM group (**Figure 4**).

Echocardiography (UCG) was performed to evaluate cardiac function of MI mice at 3 days, 1 week, and 4 weeks (Table S4) after antagomiRs treatment. Mice from both antagomiR-210 group and antagomiR_MM group exhibited significantly impaired cardiac functional at 3 days after surgery. There was no noticeable difference observed between the two groups at 3 days after surgery. However, the antagomiR-210 group demonstrated improved percent ejection fraction (%EF), fractional shortening (%FS), left ventricular (LV) end-systolic diameter (LVESD) and end-diastolic diameter (LVEDD) in antagomiR_MM group 1 week after antagomiRs treatment. And, this improvement was sustained over 4 weeks after antagomiRs treatment. In addition to UCG, hemodynamic analysis revealed a higher systolic blood pressure in antagomiR-210 group than antagomiR_MM group. The antagomiR-210 group also demonstrated higher diastolic blood pressure and lower heart rate compared to antagomiR_MM group though no statistically significant difference was found. Furthermore, we observed no significant difference in cardiac function between antagomiR-210-treated normal hearts and antagomiR_MM-treated normal hearts, suggesting that miR-210 knockdown does not affect cardiac function under non-surgical conditions.

Heart undergoes structural remodeling after infarction, resulting in a more spherical shape. The rates of overall survival of AntagomiR_210 group were significantly higher than those of AntagomiR_MM group at 15 days after AntagomiRs treatment (data not shown, 90% versus 70%). Hearts from antagomiR-210 group showed less spherical shape than those from antagomiR_MM 60 days after MI,

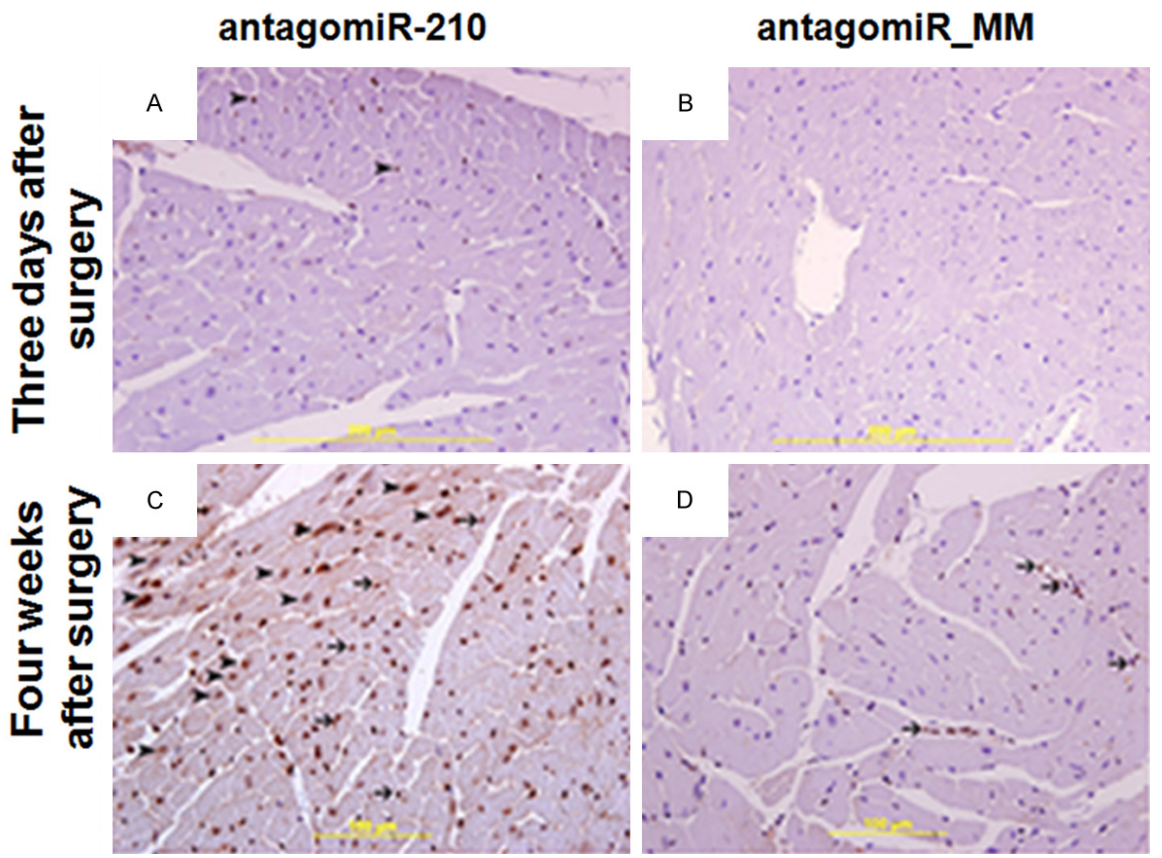

Figure 4. HIF1α expression of the heart of MI mice with treatment of antagomiRs. A & B. The expression of HIF1α in the nuclei of cardiomyocytes was detected in three-day MI mice heart with treatment of antagomiR-210. C & D. Four weeks of MI when treatment with antagomiR-210 relative to antagomiR_MM group. Streptavidin- biotin immunoperoxidase method was used.

reflecting attenuated global cardiac remodeling in mice treated with antagomiR-210. Ventricular morphology was assessed using three blocks (base, mid region and apex) of each heart and averaged (**Figure 5A**). Analysis of trichrome-stained heart cross-sections clearly showed that the infarct size was significantly reduced in mice treated with antagomiR-210 compared to antagomiR_MM group (**Figure 5B**), indicating that LV remodelling is improved by miR-210 under expression.

Discussion

Examination of global mRNA and miRNA expression profiles in AMI patients may provide novel insights into the pathogenesis of myocardial infarction-associated complications. Our primary goal was to determine the putative relationships between dysregulated genes and regulating miRNAs in AMI patients. We have observed a substantial number of dysregulated genes, particularly those genes involved in the biological processes such as cell signaling/communication, cell/organism defense and cell structure/motility, in the infarcted heart tissues derived from AMI patients. The contribution of miRNAs in regulating these differential genes was also demonstrated. There were 9 miRNAs up-regulated and 3 miRNAs down-regulated in AMI patients, which were found to potentially regulate the dysregulated mRNA in AMI patients (Table S4). The relationships between miRNAs and those dysregulated genes in the context of AMI warrant further investigation, and may serve as novel therapeutic targets in MI-associated complications.

In recent studies, miRNAs were identified as novel regulators and modifiers of cardiac development and function [28]. For instance, miRNA-21 was up regulated in the myocardium during the early phase of infarction and then controls cardiac fibrosis in response to cardiac overload

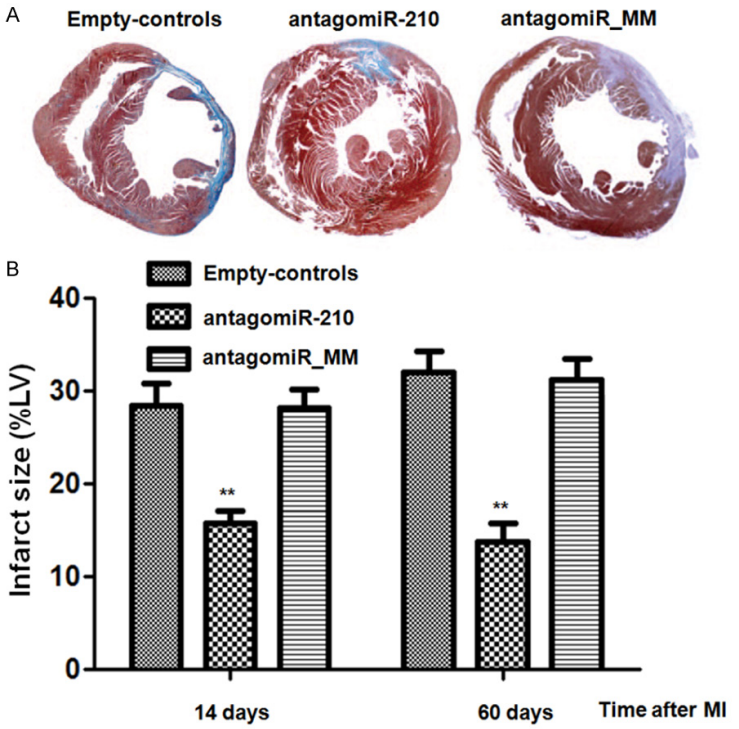

Figure 5. AntagomiR-210 preserves cardiac function after myocardial infarction. A. Masson trichrome staining of heart cross sections. B. Infarct size. n=6-10 per group. Comparison of parameters between groups was performed by unpaired Student's t test.

[29]. In this study, our findings demonstrated that 20 miRNAs were significantly up regulated and 8 miRNAs were down regulated in the AMI patients. We will validate, in future, the dysregulated miRNAs in AMI pathophysiology using a larger AMI cohort. Studies from MI animal model have been demonstrated that miRNAs from endothelial and smooth muscle cells which involved in plaque rupture and vessel injury, thrombocytes in aggregation, and inflammatory cells significantly represented the pathogenic role during development of MI [30, 31]. In addition, miR-145 was found to be involved in neointima repair in response to vascular injury, regulating cytoskeletal components and migratory activity of smooth muscle cells [32]. One may raise the question that the miRNA expression in human myocardium appears to vary drastically demonstrating about 1000-fold differentials (including hsa-miR-210) in infarcted human hearts and at least 100-fold differences in non-infarcted hearts (**Figure 2**). The relative expression levels of miR-210 in mouse hearts vary just minimally (less than 1.2-fold, **Figure 4**). This suggests that miR-210 may play different roles in human and mouse myocardium. That is why the success with antagomiR-210 (reduction in infarct size, bigger ejection fraction) in mice may not at all help humans. We can't exclude significant molecular heterogeneity within the AMI cluster because of different medical treatment or clinical course. Distinct subtypes of myocardial infarction patients with specific gene expression signature need to be established so that individual treatment can be practiced. That is to say antagomiR-210 may not function in all MI patients, but it would benefit for subtype of AMI patients with high expression of miR210 in myocardium. Further clinical study with a larger population will be needed on this issue.

HIF1α plays different roles in cardiac tissue [33]. Accumulation of HIF1α in cardiomyocytes was demonstrated to reduced contractility in adult and deterioration of ventricular function [34, 35]. In addition, over expression of HIF1α attenuated cardiac dysfunction following MI probably due to an increase in blood perfusion and glycolysis and reduction of apoptosis [34, 35]. In response to cardiac hypoxia, bone marrow cells in peripheral blood would home to the site of injury and cardiac progenitor cells that reside in the myocardium were then activated. These recruited cells can regenerate damaged tissue by differentiating into endothelial cells, smooth muscle cells, and cardiac myocytes. HIF1α was also sensitive to hypoxia and rapidly degraded by the ubiquitin proteasomal pathway under normoxic conditions. Decreased tissue oxygen causes altered availability of HIF1α to the von Hippel-Lindau protein and ubiquitination, blocking its degradation, which results in nuclear accumulation of HIF1α protein and enhancement of its transcriptional activity through binding to enhancer elements in target genes that include vascular endothelial growth factor, inducible nitric oxide synthase, erythropoietin, and phosphoglycerate kinase. In our current study, we further examined that miR-210 dramatically decreased in the antagomiR-210 group 24 hrs after infarction

and maintained thereafter 20-25% of the miR-210 levels in the AntagomiR group over the 44-day period (Figure S1). However, there was a higher nuclear expression of HIF1α by cardiac myocytes and endothelial cells after four weeks of MI when treatment with antagomiR-210 relative to antagomiR_MM group (**Figure 4C** and **4D**). In addition, under expression of miR-210 by one week after antagomiRs treatment demonstrated improved per cent ejection fraction (%EF), fractional shortening (%FS), left ventricular (LV) end-systolic diameter (LVESD) and end-diastolic diameter (LVEDD). Hearts from antagomiR-210 group showed less spherical shape than those from antagomiR_MM 60 days after MI (**Figure 5A** and **5B**), indicating under expression of miR-210 improve heart function after MI. One may raise a question on the relationship between human AMI samples and the mice MI samples. The clinical data in human was from acute (presumably) death following a myocardial infarction (MI), while the murine studies were more subacute. The mechanisms of death acutely from MI (shock or arrhythmia) are very different from the more subacute to chronic changes described (ventricular remodeling). Since we don't have the data showing either acute survival is better in post-infarct mice with miR-210, or that chronic heart failure human patients demonstrate similar derangements, the link between the human and murine parts of our study remain unclear.

We recognize that there are some limitations to this exploratory study. Firstly, the sample size was still small. Secondly, it is not yet firmly established on the standard method of statistical analysis on miRNA-mRNA pairs. Finally, we have not examined other miRNAs (~1100). Thus identification of miRNomes in-depth by miRNA-seq may reveal the more miRNAs involved in AMI. Another limitation is that the target prediction of miR-210 demonstrated many other potential targets. Therefore, we cannot exclude the possibility of other potential targets for miR-210 that may have an impact on the observed myocardial protection after antagomir-210 injection.

In conclusion, our study demonstrated that a substantial proportion of the pathogenic miRNA-mRNA pairs in AMI patients. Knockdown of miR-210 expression would improve the cardiac function in MI animal model. Therefore, our findings suggest the pathogenic miRNA-mRNA pairs may have important implications for the treatment of cardiac pathologies consequent to human myocardial infarction.

Acknowledgements

This study is supported by the Medical Scientific Research Foundation of Zhejiang Province, China (Grant No. 2013KYB031), the National Natural Science Foundation of China (Grant No. 81200113), the Fundamental Research Funds for the Central Universities (Grant No. 2014FZA7014), the Science and Technology Planning Project of Zhejiang Province, China (Grant No. 2014C37002), the Natural Science Foundation of Zhejiang Province, China (Grant No. LQ15H060003) and the Natural Science Foundation of Zhejiang Province, China (Grant No. LY15H020005). Grant from Science Technology Department of Zhejiang Province (2013R10049, 2013C03043-4). The authors thank all the AMI patients who participated in this study and the staff from Second Affiliated Hospital, College of Medicine, Zhejiang University during the study.

Disclosure of conflict of interest

None to disclose.

Address correspondence to: Jian'an Wang and Yaping Wang, Department of Cardiology, Second Affiliated Hospital, College of Medicine, Zhejiang University, Hangzhou, 310009, PR China; Key Lab of Cardiovascular Disease, Second Affiliated Hospital, College of Medicine, Zhejiang University, Hangzhou, 310009, PR China. E-mail: jian_an_wang@yahoo.com (JAW); yapingwang01@gmail.com (YPW)

References

[1] Ibrahim AW, Riddell TC and Devireddy CM. Acute Myocardial Infarction. Crit Care Clin 2014; 30: 341-364.

[2] Bainey KR and Armstrong PW. Clinical perspectives on reperfusion injury in acute myocardial infarction. Am Heart J 2014; 167: 637-645.

[3] Barron HV, Harr SD, Radford MJ, Wang Y and Krumholz HM. The association between white blood cell count and acute myocardial infarction mortality in patients > or =65 years of age: findings from the cooperative cardiovascular project. J Am Coll Cardiol 2001; 38: 1654-1661.

[4] Mueller C, Neumann FJ, Perruchoud AP and Buettner HJ. White blood cell count and long term mortality after non-ST elevation acute

coronary syndrome treated with very early revascularisation. Heart 2003; 89: 389-392.
[5] Bartel DP. MicroRNAs: target recognition and regulatory functions. Cell 2009; 136: 215-233.
[6] Chen JF, Murchison EP, Tang R, Callis TE, Tatsuguchi M, Deng Z, Rojas M, Hammond SM, Schneider MD, Selzman CH, Meissner G, Patterson C, Hannon GJ and Wang DZ. Targeted deletion of Dicer in the heart leads to dilated cardiomyopathy and heart failure. Proc Natl Acad Sci U S A 2008; 105: 2111-2116.
[7] Rao PK, Toyama Y, Chiang HR, Gupta S, Bauer M, Medvid R, Reinhardt F, Liao R, Krieger M, Jaenisch R, Lodish HF and Blelloch R. Loss of cardiac microRNA-mediated regulation leads to dilated cardiomyopathy and heart failure. Circ Res 2009; 105: 585-594.
[8] Ikeda S, Kong SW, Lu J, Bisping E, Zhang H, Allen PD, Golub TR, Pieske B and Pu WT. Altered microRNA expression in human heart disease. Physiol Genomics 2007; 31: 367-373.
[9] Matkovich SJ, Van Booven DJ, Youker KA, Torre-Amione G, Diwan A, Eschenbacher WH, Dorn LE, Watson MA, Margulies KB and Dorn GW 2nd. Reciprocal regulation of myocardial microRNAs and messenger RNA in human cardiomyopathy and reversal of the microRNA signature by biomechanical support. Circulation 2009; 119: 1263-1271.
[10] Thum T, Galuppo P, Wolf C, Fiedler J, Kneitz S, van Laake LW, Doevendans PA, Mummery CL, Borlak J, Haverich A, Gross C, Engelhardt S, Ertl G and Bauersachs J. MicroRNAs in the human heart: a clue to fetal gene reprogramming in heart failure. Circulation 2007; 116: 258-267.
[11] Stanton LW, Garrard LJ, Damm D, Garrick BL, Lam A, Kapoun AM, Zheng Q, Protter AA, Schreiner GF and White RT. Altered patterns of gene expression in response to myocardial infarction. Circ Res 2000; 86: 939-945.
[12] Kiliszek M, Burzynska B, Michalak M, Gora M, Winkler A, Maciejak A, Leszczynska A, Gajda E, Kochanowski J and Opolski G. Altered gene expression pattern in peripheral blood mononuclear cells in patients with acute myocardial infarction. PLoS One 2012; 7: e50054.
[13] Van de Werf F, Bax J, Betriu A, Blomstrom-Lundqvist C, Crea F, Falk V, Filippatos G, Fox K, Huber K, Kastrati A, Rosengren A, Steg PG, Tubaro M, Verheugt F, Weidinger F and Weis M. Management of acute myocardial infarction in patients presenting with persistent ST-segment elevation: the Task Force on the Management of ST-Segment Elevation Acute Myocardial Infarction of the European Society of Cardiology. Eur Heart J 2008; 29: 2909-2945.
[14] Irizarry RA, Hobbs B, Collin F, Beazer-Barclay YD, Antonellis KJ, Scherf U and Speed TP. Exploration, normalization, and summaries of high density oligonucleotide array probe level data. Biostatistics 2003; 4: 249-264.
[15] Duan S, Zhang W, Bleibel WK, Cox NJ and Dolan ME. SNPinProbe_1.0: a database for filtering out probes in the Affymetrix GeneChip human exon 1.0 ST array potentially affected by SNPs. Bioinformation 2008; 2: 469-470.
[16] Pruitt KD, Tatusova T and Maglott DR. NCBI reference sequences (RefSeq): a curated non-redundant sequence database of genomes, transcripts and proteins. Nucleic Acids Res 2007; 35: D61-65.
[17] Tusher VG, Tibshirani R and Chu G. Significance analysis of microarrays applied to the ionizing radiation response. Proc Natl Acad Sci U S A 2001; 98: 5116-5121.
[18] Huang da W, Sherman BT and Lempicki RA. Systematic and integrative analysis of large gene lists using DAVID bioinformatics resources. Nat Protoc 2009; 4: 44-57.
[19] Dennis G Jr, Sherman BT, Hosack DA, Yang J, Gao W, Lane HC and Lempicki RA. DAVID: Database for Annotation, Visualization, and Integrated Discovery. Genome Biol 2003; 4: P3.
[20] Kanehisa M, Goto S, Kawashima S, Okuno Y and Hattori M. The KEGG resource for deciphering the genome. Nucleic Acids Res 2004; 32: D277-280.
[21] Ashburner M, Ball CA, Blake JA, Botstein D, Butler H, Cherry JM, Davis AP, Dolinski K, Dwight SS, Eppig JT, Harris MA, Hill DP, Issel-Tarver L, Kasarskis A, Lewis S, Matese JC, Richardson JE, Ringwald M, Rubin GM and Sherlock G. Gene ontology: tool for the unification of biology. The Gene Ontology Consortium. Nat Genet 2000; 25: 25-29.
[22] Kainkaryam RM, Bruex A, Woolf PJ and Schiefelbein J. Smart pooling of mRNA samples for efficient transcript profiling. Methods Mol Biol 2012; 876: 189-194.
[23] Velu CS and Grimes HL. Utilizing antagomiR (antisense microRNA) to knock down microRNA in murine bone marrow cells. Methods Mol Biol 2012; 928: 185-195.
[24] Chen C, Ridzon DA, Broomer AJ, Zhou Z, Lee DH, Nguyen JT, Barbisin M, Xu NL, Mahuvakar VR, Andersen MR, Lao KQ, Livak KJ and Guegler KJ. Real-time quantification of microRNAs by stem-loop RT-PCR. Nucleic Acids Res 2005; 33: e179.
[25] Tang F, Hajkova P, Barton SC, O'Carroll D, Lee C, Lao K and Surani MA. 220-plex microRNA expression profile of a single cell. Nat Protoc 2006; 1: 1154-1159.
[26] Griffiths-Jones S, Saini HK, van Dongen S and Enright AJ. miRBase: tools for microRNA ge-

nomics. Nucleic Acids Res 2008; 36: D154-158.
[27] Betel D, Koppal A, Agius P, Sander C and Leslie C. Comprehensive modeling of microRNA targets predicts functional non-conserved and non-canonical sites. Genome Biol 2010; 11: R90.
[28] Meder B, Katus HA and Rottbauer W. Right into the heart of microRNA-133a. Genes Dev 2008; 22: 3227-3231.
[29] Dong S, Cheng Y, Yang J, Li J, Liu X, Wang X, Wang D, Krall TJ, Delphin ES and Zhang C. MicroRNA expression signature and the role of microRNA-21 in the early phase of acute myocardial infarction. J Biol Chem 2009; 284: 29514-29525.
[30] Ono K, Matsumori A, Shioi T, Furukawa Y and Sasayama S. Cytokine gene expression after myocardial infarction in rat hearts: possible implication in left ventricular remodeling. Circulation 1998; 98: 149-156.
[31] Guo CY, Yin HJ, Jiang YR, Xue M, Zhang L and Shi da Z. [Differential gene expression profile in ischemic myocardium of Wistar rats with acute myocardial infarction: the study on gene construction, identification and function]. Beijing Da Xue Xue Bao 2008; 40: 251-257.
[32] Xin M, Small EM, Sutherland LB, Qi X, McAnally J, Plato CF, Richardson JA, Bassel-Duby R and Olson EN. MicroRNAs miR-143 and miR-145 modulate cytoskeletal dynamics and responsiveness of smooth muscle cells to injury. Genes Dev 2009; 23: 2166-2178.
[33] Majmundar AJ, Wong WJ and Simon MC. Hypoxia-inducible factors and the response to hypoxic stress. Mol Cell 2010; 40: 294-309.
[34] Bekeredjian R, Walton CB, MacCannell KA, Ecker J, Kruse F, Outten JT, Sutcliffe D, Gerard RD, Bruick RK and Shohet RV. Conditional HIF-1alpha expression produces a reversible cardiomyopathy. PLoS One 2010; 5: e11693.
[35] Minamishima YA, Moslehi J, Bardeesy N, Cullen D, Bronson RT and Kaelin WG Jr. Somatic inactivation of the PHD2 prolyl hydroxylase causes polycythemia and congestive heart failure. Blood 2008; 111: 3236-3244.

Table S1. Clinical features of subjects in the study

Clinical features	AMI groups	Healthy groups
Men/Women	13/10	13/10
Age	57±11	60±8
Anterior myocardial infarction	12 (52%)	NA
Hypertension	10 (43%)	0
Diabetes	5 (22%)	0
Current smokers	8 (35%)	6 (26%)
Previous myocardial infarction	2 (8%)	NA
Body Mass Index (BMI)	30±3	31±5
Treatment		
Aspirin	23 (100%)	NA
Clopidogrel	23 (100%)	NA
Statin	23 (100%)	NA
Beta blocker	23 (100%)	NA
ACE inhibitor	18 (78%)	NA
Heparin (UFH or LMWH)	23 (100%)	NA

Table S2. The dysregulated genes in patients with acute myocardial infarction

Gene Symbol	Gene Title	Fold Change	*p*-value
SOCS3	suppressor of cytokine signaling 3	3.18	2.04E-06
TMEM176A	transmembrane protein 176A	2.91	4.28E-02
HP	Haptoglobin	2.61	1.66E-01
STAB1	stabilin 1	2.59	1.36E-07
FAM20A	family with sequence similarity 20, member A	2.56	8.64E-03
EGR1	early growth response 1	2.54	1.67E+00
ASGR2	asialoglycoprotein receptor 2	2.54	6.48E-07
GSTM1	glutathione S-transferase mu 1	2.49	3.90E-03
TCN2	transcobalamin II	2.39	5.60E-04
DYSF	dysferlin, limb girdle muscular dystrophy 2B (autosomal recessive)	2.30	1.56E-03
RNASE2	ribonuclease, RNase A family, 2 (liver, eosinophil-derived neurotoxin)	2.30	5.32E-03
LGALS9	lectin, galactoside-binding, soluble, 9	2.29	3.85E-05
mTOR	mechanistic target of rapamycin (serine/threonine kinase)	2.28	1.00E-05
CA5BP1	carbonic anhydrase VB pseudogene 1	2.27	3.46E-08
IL12A	interleukin 12A	2.26	8.60E-11
ZFP36	zinc finger protein 36, C3H type, homolog (mouse)	2.25	2.43E-07
AQP9	aquaporin 9	2.25	1.99E-03
HBEGF	heparin-binding EGF-like growth factor	2.25	6.96E-03
CYP27A1	cytochrome P450, family 27, subfamily A, polypeptide 1	2.24	3.16E-04
LOC441081	POM121 membrane glycoprotein (rat) pseudogene	2.24	2.81E-03
PPARG	peroxisome proliferator-activated receptor gamma	2.22	7.36E-05
GPR180	G protein-coupled receptor 180	2.22	4.36E-12
KCTD12	potassium channel tetramerisation domain containing 12	2.19	2.28E-12
LOC441081	POM121 membrane glycoprotein (rat) pseudogene	2.19	0.004
MLF2	myeloid leukemia factor 2	2.18	0.052
RNASE1	ribonuclease, RNase A family, 1 (pancreatic)	2.18	0.018
LOC441081	POM121 membrane glycoprotein (rat) pseudogene	2.17	0.025
BCL3	B-cell CLL/lymphoma 3	2.16	0.011
FCGR1A	Fc fragment of IgG, high affinity Ia, receptor (CD64)	2.15	0.019
FAM20C	family with sequence similarity 20, member C	2.13	0.020
FCGR1A	Fc fragment of IgG, high affinity Ia, receptor (CD64)	2.12	0.050
RAB1B	RAB1B, member RAS oncogene family	2.12	0.023

SIGLEC7/SIGLEC9	sialic acid binding Ig-like lectin 7	2.12	0.012
LILRB4	leukocyte immunoglobulin-like receptor, subfamily B (with TM and ITIM domains), member 4	2.11	0.015
CD151	CD151 molecule (Raph blood group)	2.11	0.029
FCGR1A	Fc fragment of IgG, high affinity Ia, receptor (CD64)	2.11	0.034
CSF3R	colony stimulating factor 3 receptor (granulocyte)	2.09	0.082
EGR2	early growth response 2	2.09	0.010
PADI2	peptidyl arginine deiminase, type II	2.08	0.084
SASH1	SAM and SH3 domain containing 1	2.08	0.019
LGALS9B	lectin, galactoside-binding, soluble, 9B	2.08	0.017
ROGDI	rogdi homolog (Drosophila)	2.08	0.039
LGALS9B	lectin, galactoside-binding, soluble, 9B	2.06	0.033
CYP1B1	cytochrome P450, family 1, subfamily B, polypeptide 1	2.06	0.014
ZNF280C	zinc finger protein 280C	2.05	0.020
HSPA1A/HSPA1B	heat shock 70 kDa protein 1A	2.05	0.042
NFE2	nuclear factor (erythroid-derived 2), 45 kDa	2.05	0.076
HSPA1A/HSPA1B	heat shock 70 kDa protein 1A	2.05	0.070
HSPA1A/HSPA1B	heat shock 70 kDa protein 1A	2.05	0.070
RASGRP4	RAS guanyl releasing protein 4	2.04	0.050
GPSM3	G-protein signaling modulator 3	2.04	0.084
CTSD	cathepsin D	2.03	0.028
FLOT2	flotillin 2	2.03	0.052
FAM101B	family with sequence similarity 101, member B	2.03	0.078
THBD	Thrombomodulin	2.02	0.000
GSK3A	glycogen synthase kinase 3 alpha	2.02	0.028
LSP1 (includes EG:16985)	lymphocyte-specific protein 1	2.01	0.034
C1QC	complement component 1, q subcomponent, C chain	2.01	0.077
CPNE2	copine II	2.00	0.098
CCDC97	coiled-coil domain containing 97	2.00	0.031
PLSCR3	phospholipid scramblase 3	2.00	0.036
DOK3	docking protein 3	2.00	0.001
IL1RN	interleukin 1 receptor antagonist	2.00	0.042
ZNF385A	zinc finger protein 385A	2.00	0.002
SIGLEC7/SIGLEC9	sialic acid binding Ig-like lectin 7	1.99	0.002
GNG11	guanine nucleotide binding protein (G protein), gamma 11	-2.10	2.04E-07
IGJ	immunoglobulin J polypeptide, linker protein for immunoglobulin alpha and mu polypeptides	-2.08	4.28E-03
C15orf54	chromosome 15 open reading frame 54	-2.02	1.66E-02
PDE5A	phosphodiesterase 5A, cGMP-specific	-1.90	1.36E-08
ENKUR	enkurin, TRPC channel interacting protein	-1.89	8.64E-04
MMD	monocyte to macrophage differentiation-associated	-1.80	1.67E-01
HSPC159	galectin-related protein	-1.78	6.48E-08
KLRF1	killer cell lectin-like receptor subfamily F, member 1	-1.78	3.90E-03
PRKAR2B	protein kinase, cAMP-dependent, regulatory, type II, beta	-1.68	5.60E-05
ITGB3	integrin, beta 3 (platelet glycoprotein IIIa, antigen CD61)	-1.61	1.56E-03
PPBP	pro-platelet basic protein (chemokine (C-X-C motif) ligand 7)	-1.61	5.32E-03
RAB27B	RAB27B, member RAS oncogene family	-1.60	3.85E-06
F13A1	coagulation factor XIII, A1 polypeptide	-1.59	1.00E-06
TCF7	transcription factor 7, T cell specific	-1.57	3.46E-09
CDK13	cyclin-dependent kinase 13	-1.53	8.60E-12
DAB2	disabled homolog 2, mitogen-responsive phosphoprotein (Drosophila)	-1.52	2.43E-08
SELP	selectin P (granule membrane protein 140 kDa, antigen CD62)	-1.51	1.99E-03
BANK1	B-cell scaffold protein with ankyrin repeats 1	-1.48	6.96E-03
MFAP3L	microfibrillar-associated protein 3-like	-1.47	3.16E-05
SPARC	secreted protein, acidic, cysteine-rich (osteonectin)	-1.47	2.81E-04
ZNF542	zinc finger protein 542	-1.46	7.36E-06
SH2D1B	SH2 domain containing 1B	-1.44	4.36E-13
P2RY12	purinergic receptor P2Y, G-protein coupled, 12	-1.44	2.28E-13
NF1	neurofibromin 1	-1.40	3.94E-04

CCL8	chemokine (C-C motif) ligand 8	-1.40	5.20E-25
KLRB1	killer cell lectin-like receptor subfamily B, member 1	-1.39	1.07E-03
MMRN1	multimerin 1	-1.36	2.46E-04
LTBP1	latent transforming growth factor beta binding protein 1	-1.33	1.13E-10
RGS18	regulator of G-protein signaling 18	-1.32	1.86E-02
AKT3	v-akt murine thymoma viral oncogene homolog 3 (protein kinase B, gamma)	-1.31	2.05E-07
NEXN	nexilin (F actin binding protein)	-1.31	5.00E-02
MEIS1	Meis homeobox 1	-1.29	2.34E-09
TREML1	triggering receptor expressed on myeloid cells-like 1	-1.28	1.24E-06
LOC147727	hypothetical LOC147727	-1.27	1.47E-05
CD1C	CD1c molecule	-1.26	2.88E-04
LY86	lymphocyte antigen 86	-1.24	3.36E-02
CD9	CD9 molecule	-1.24	8.16E-07
CCR4	chemokine (C-C motif) receptor 4	-1.22	1.00E-02
KIF2A	kinesin heavy chain member 2A	-1.20	8.36E-03
SCARNA6	small Cajal body-specific RNA 6	-1.17	1.93E-05
ANKRD32	ankyrin repeat domain 32	-1.17	1.72E-05
SNORD105	small nucleolar RNA, C/D box 105	-1.17	3.88E-06
TAF1D	TATA box binding protein (TBP)-associated factor, RNA polymerase I, D, 41 kDa	-1.16	3.32E-05
CLC	Charcot-Leyden crystal protein	-1.16	1.37E-03
SNORA20	small nucleolar RNA, H/ACA box 20	-1.14	1.99E-11
GPR128	G protein-coupled receptor 128	-1.13	4.20E-09
SNORA24	small nucleolar RNA, H/ACA box 24	-1.12	7.56E-05
SNHG12	small nucleolar RNA host gene 12 (non-protein coding)	-1.12	6.96E-09
KLRC1	killer cell lectin-like receptor subfamily C, member 1	-1.11	6.96E-09
GIMAP2	GTPase, IMAP family member 2	-1.10	5.04E-07
SAV1	salvador homolog 1 (Drosophila)	-1.09	8.40E-13
FTL	ferritin, light polypeptide	-1.08	2.84E-11
GUCY1B3	guanylate cyclase 1, soluble, beta 3	-1.08	1.32E-14
NELL2	NEL-like 2 (chicken)	-1.08	5.20E-12
LYRM7	Lyrm7 homolog (mouse)	-1.08	7.76E-12
TC2N	tandem C2 domains, nuclear	-1.08	3.46E-06
TPMT	thiopurine S-methyltransferase	-1.07	5.92E-02
PID1	phosphotyrosine interaction domain containing 1	-1.07	2.82E-21
BTLA	B and T lymphocyte associated	-1.07	1.15E-08
MOBKL1A	MOB1, Mps One Binder kinase activator-like 1A (yeast)	-1.06	3.39E-10
TXK	TXK tyrosine kinase	-1.05	7.68E-05
NDUFA5	NADH dehydrogenase (ubiquinone) 1 alpha subcomplex, 5, 13 kDa	-1.04	9.76E-08
NAP1L1	nucleosome assembly protein 1-like 1	-1.04	3.13E-11
RALGPS2	Ral GEF with PH domain and SH3 binding motif 2	-1.03	3.56E-06
GUCY1A3	guanylate cyclase 1, soluble, alpha 3	-1.03	1.43E-09
PTGDR	prostaglandin D2 receptor (DP)	-1.03	4.16E-05
ZNF141	zinc finger protein 141	-1.02	2.42E-06
SEP11.	septin 11	-1.02	2.44E-06
LRRC8B	leucine rich repeat containing 8 family, member B	-1.01	8.12E-03
FGD6	FYVE, RhoGEF and PH domain containing 6	-1.01	1.28E-07
BET1	blocked early in transport 1 homolog (S. cerevisiae)	-1.01	2.98E-03
RWDD4A	RWD domain containing 4A	-1.01	4.04E-08
DYNLL1	dynein, light chain, LC8-type 1	-1.01	5.40E-08
PLEKHA1	pleckstrin homology domain containing, family A (phosphoinositide binding specific) member 1	-1.01	1.47E-09
NPCDR1	nasopharyngeal carcinoma, down-regulated 1	-1.00	1.59E-05
TTC39B	tetratricopeptide repeat domain 39B	-1.00	1.46E-03
IL7R	interleukin 7 receptor	-1.00	1.61E-11
SDAD1	SDA1 domain containing 1	-1.00	1.87E-07
JAM3	junctional adhesion molecule 3	-0.99	6.28E-06
PARP15	poly (ADP-ribose) polymerase family, member 15	-0.99	6.48E-03

PREPL	prolyl endopeptidase-like	-0.99	3.83E-08
RPE	ribulose-5-phosphate-3-epimerase	-0.99	1.30E-09
PYHIN1	pyrin and HIN domain family, member 1	-0.98	1.48E-09
ITGB3BP	integrin beta 3 binding protein (beta3-endonexin)	-0.98	1.89E-06
LYRM5	LYR motif containing 5	-0.98	1.35E-10
CD226	CD226 molecule	-0.98	1.88E-02
C7orf58	chromosome 7 open reading frame 58	-0.98	9.28E-02
LRBA	LPS-responsive vesicle trafficking, beach and anchor containing	-0.98	9.28E-02
RPS24	ribosomal protein S24	-0.97	9.28E-02
DNAJC8	DnaJ (Hsp40) homolog, subfamily C, member 8	-0.97	9.28E-02
FAM164A	family with sequence similarity 164, member A	-0.97	4.84E-03
CA2	carbonic anhydrase II	-0.97	4.84E-03
ARAP2	ArfGAP with RhoGAP domain, ankyrin repeat and PH domain 2	-1.95	3.59E-09
F2R	coagulation factor II (thrombin) receptor	-1.95	1.54E-04
FANCL	Fanconi anemia, complementation group L	-1.95	2.54E-06
RABGGTB	Rab geranylgeranyltransferase, beta subunit	-1.95	4.52E-07
HIST1H4A	histone cluster 1, H4a	-1.96	2.38E-02
KPNA5	karyopherin alpha 5 (importin alpha 6)	-1.96	8.56E-10
CCL4	chemokine (C-C motif) ligand 4	-1.96	3.40E-04
MS4A2	membrane-spanning 4-domains, subfamily A, member 2 (Fc fragment of IgE, high affinity I, receptor for; beta polypeptide)	-1.96	2.24E-04
SYNE1	spectrin repeat containing, nuclear envelope 1	-1.97	7.04E-05
TARP	TCR gamma alternate reading frame protein	-1.97	7.76E-03
FAM169A	family with sequence similarity 169, member A	-1.97	1.70E-04
PPBP	pro-platelet basic protein (chemokine (C-X-C motif) ligand 7)	-1.97	4.08E-03
SNORD94	small nucleolar RNA, C/D box 94	-1.97	1.21E-08
SYTL2	synaptotagmin-like 2	-1.98	4.76E-04
ENPP4	ectonucleotide pyrophosphatase/phosphodiesterase 4 (putative)	-1.98	3.55E-08
PDE5A	phosphodiesterase 5A, cGMP-specific	-1.98	5.28E-03
RPL13A	ribosomal protein L13a	-1.98	7.20E-06
GK5	glycerol kinase 5 (putative)	-1.99	3.94E-06
RNU4ATAC	RNA, U4atac small nuclear (U12-dependent splicing)	-1.99	9.28E-07
BRK1	BRICK1, SCAR/WAVE actin-nucleating complex subunit	-1.99	3.50E-10
EPB41L4A	erythrocyte membrane protein band 4.1 like 4A	-2.00	7.76E-02
SAMD3	sterile alpha motif domain containing 3	-2.00	2.36E-05
FGFBP2	fibroblast growth factor binding protein 2	-2.00	8.80E-02
SNORA1	small nucleolar RNA, H/ACA box 1	-2.00	9.96E-06
VTRNA1-1	vault RNA 1-1	-2.00	2.61E-04
CNOT6L	CCR4-NOT transcription complex, subunit 6-like	-2.01	1.44E-11
SLFN13	schlafen family member 13	-2.01	3.78E-07
SNORA19	small nucleolar RNA, H/ACA box 19	-2.02	4.12E-09
MMRN1	multimerin 1	-2.02	5.40E-03
CCL4	chemokine (C-C motif) ligand 4	-2.02	5.76E-04
HIF1A	hypoxia inducible factor 1, alpha subunit	-2.02	5.76E-04
TAF1D	TATA box binding protein (TBP)-associated factor, RNA polymerase I, D, 41 kDa	-2.02	1.30E-05
RMRP	RNA component of mitochondrial RNA processing endoribonuclease	-2.03	3.21E-07
LLPH	LLP homolog, long-term synaptic facilitation (Aplysia)	-2.03	2.27E-04
DEFA1	defensin, alpha 1	-2.03	5.40E-05
CDYL	chromodomain protein, Y-like	-2.04	2.93E-05
EIF2C4	eukaryotic translation initiation factor 2C, 4	-2.04	6.04E-03
SNORD54	small nucleolar RNA, C/D box 54	-2.04	2.20E-02
SNORA68	small nucleolar RNA, H/ACA box 68	-2.05	1.59E-05
KLRC3	killer cell lectin-like receptor subfamily C, member 3	-2.06	2.54E-06
SNORD1C	small nucleolar RNA, C/D box 1C	-2.06	3.06E-04
SCARNA10	small Cajal body-specific RNA 10	-2.06	2.75E-05
KLRC4	killer cell lectin-like receptor subfamily C, member 4	-2.06	1.33E-03
RNU4-2	RNA, U4 small nuclear 2	-2.07	2.66E-04

SCARNA7	small Cajal body-specific RNA 7	-2.07	8.76E-10
CPNE3	copine III	-2.07	2.85E-03
TGFBR2	transforming growth factor, beta receptor II	-2.07	1.40E-07
SNHG3	small nucleolar RNA host gene 3 (non-protein coding)	-2.07	1.18E-01
CDK19	cyclin-dependent kinase 19	-2.07	1.08E-04
CCL16	chemokine (C-C motif) ligand 16	-2.07	5.84E-02
SNORD60	small nucleolar RNA, C/D box 60	-2.07	1.86E-03
SNORD82	small nucleolar RNA, C/D box 82	-2.08	1.37E-06
MS4A3	membrane-spanning 4-domains, subfamily A, member 3 (hematopoietic cell-specific)	-2.08	1.11E-06
SNORD14E	small nucleolar RNA, C/D box 14E	-2.08	5.12E-05
KLRG1	killer cell lectin-like receptor subfamily G, member 1	-2.08	2.11E-03
NCKAP1	NCK-associated protein 1	-2.09	2.01E-04
JAM3	junctional adhesion molecule 3	-2.09	9.92E-03
SCARNA17	small Cajal body-specific RNA 17	-2.10	1.32E-07
RPL7A	ribosomal protein L7a	-2.10	2.54E-09
SNORD59B	small nucleolar RNA, C/D box 59B	-2.10	2.09E-09
KLRAP1	killer cell lectin-like receptor subfamily A pseudogene 1	-2.12	1.25E-03

Table S3. Differential miRNAs between AMI patients vs. non-AMI controls

AMI vs. Control	miRNA	Fold change	Adjusted P
Up-regulated	hsa-miR-1	2.786	0.021
	hsa-miR-186	7.251	0.014
	hsa-miR-210	3.280	0.013
	hsa-miR-20a	3.363	0.014
	hsa-miR-208a	3.423	0.011
	hsa-miR-150	2.848	0.000
	hsa-miR-125b	5.076	0.003
	hsa-miR-135b	3.454	0.013
	hsa-miR-137	2.976	0.018
	hsa-miR-148b	2.953	0.008
	hsa-miR-184	3.809	0.001
	hsa-miR-190	2.799	0.006
	hsa-miR-199b	3.660	0.018
	hsa-miR-203	2.860	0.003
	hsa-miR-219	2.855	0.020
	hsa-miR-451	3.198	0.011
	hsa-miR-302b	9.094	0.019
	hsa-miR-335	3.703	0.018
	hsa-miR-133a	2.349	0.021
	hsa-miR-548	2.715	0.003
Down-regulated	has-let-7a	0.378	0.000
	has-miR-99a	0.298	0.020
	has-let-7f	0.382	0.009
	hsa-miR-187	0.245	0.000
	has-miR-15b	0.275	0.021
	hsa-miR-433	0.347	0.018
	hsa-miR-195	0.296	0.019
	hsa-miR-494	0.336	0.016

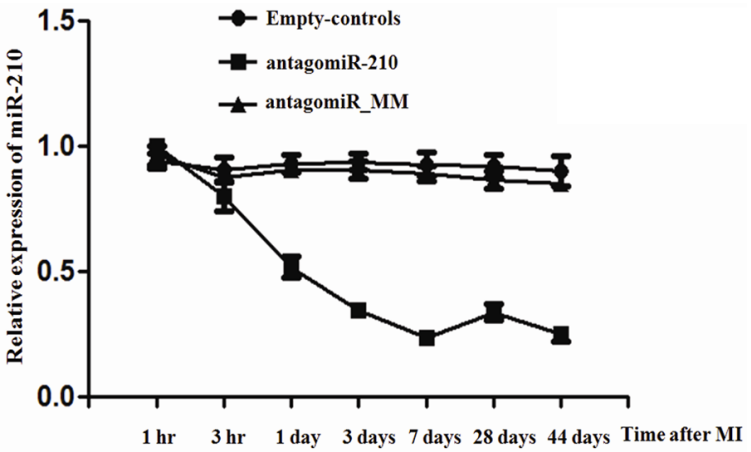

Figure S1. Expression profile of miR-210 in mice after MI. MiR-210 expression in the infarcted heart was assessed by RT-PCR at the indicated times after surgery (n=5, each time-point per group). MiR-210 expression was normalized to the U6 expression and expressed as fold change relative to non-AMI controls.

Table S4. UCG was performed 3 days, 1 week and 4 weeks after surgery

Time	Pre-injury	3 days			1 week			4 weeks		
Groups	Pre-injury	Control	antagomiR210	antagomiRMM	Control	antagomiR210	antagomiRMM	Control	antagomiR210	antagomiRMM
EF%	44.2±2.7	56.56±1.35	58.41±1.33*	55.96±1.65	43.29±3.14	47.29±2.77**	41.99±3.32	38.64±1.36	45.34±1.44**	39.61±1.21
FS%	19.75±2.22	28.14±1.18	29.34±1.25	28.84±1.48	20.33±1.52	22.17±1.58*	21.88±1.85	19.11±0.81	20.21±0.72	18.92±0.65
LVEDD (mm)	4.89±1.09	3.14±0.27	3.36±0.15	3.11±0.23	4.38±0.19	3.89±0.23**	4.26±0.24	4.97±0.33	4.14±0.22*	4.85±0.34
LVESD (mm)	4.12±0.87	2.66±0.38	2.51±0.25	2.55±0.32	3.13±0.18	3.77±0.42*	3.23±0.16	4.21±0.29	3.89±0.37*	4.13±0.26

Note: Definition of abbreviations; EF: Ejection fraction; LVEDD: LV end-diastolic diameter; LVESD: LV end-systolic diameter; %FS: percent fractional shortening. *: $P < 0.05$; **: $P < 0.01$.